Capacitance Characterization Method for Thick-Conductor Multiple Planar Ring Structures on Multiple Substrate Layers

Faton Tefiku, *Student Member, IEEE,* and Eikichi Yamashita, *Fellow, IEEE*

Abstract—**A capacitance characterization method for thick-conductor multiple planar ring structures on multiple substrates layers has been made for the first time by extending the rectangular boundary division method. The region to be considered in the analysis is divided into subregions of thick-wall cylindrical tubes in each of which Laplace's equation is solved by the method of the separation of variables. A special application scheme of the boundary conditions is devised to decrease the number of necessary equations. Numerical results are shown for circular disk and planar ring structures in comparison with other available data.**

I. Introduction

THE CAPACITANCE characterization of planar ring structures on multiple substrate layers is desirable for designing various lumped circuits elements in microwave integrated circuits. In the past, much attention was paid to circular disk structures in free space, and later to circular disks on a dielectric substrate backed by a ground plane with advent of microwave integrated circuits. The insertion of a dielectric substrate between the disk and the ground plane adds more complications in finding analytical expressions for fields. The problem of the circular disk has been studied by several authors based on Galerkin's method in the Hankel transform domain [1]–[2], the method of dual integral equations [3]–[7], and Nobel's variational method [8].

These methods have dealt with difficulties in selecting proper basis functions for the charge distribution on the disk conductor, or in carrying out the infinite integral including Bessel functions. Closed form expressions for the capacitance of the circular disk have been discussed using the fact that the fringing field of a circular disk is similar to that of a degenerated microstrip line [9]–[10], and using the method of matched asymptotic expansions [11]. A more accurate formula valid for both small and large disks has been given by Wheeler [12].

The historical background for the capacitance calculation of a circular disk capacitor together with explicit approximation expressions for the capacitance of a conductor patch of arbitrary shape has been described by Kuester [13]. The work on the capacitance of the planar ring has been rarely reported, to the author's knowledge, perhaps due to the above mentioned difficulties, although some data have been published based on Galerkin's method in the Hankel transform domain with basis functions symmetric about the mean radius [14]–[15]. Closed form expressions for the fringing fields outside and inside of a planar ring have been given based on those of degenerated microstrip lines and coupled straight lines, respectively, [10].

We have analyzed the capacitance of zero-thickness planar ring structures based on the rectangular boundary division method in a previous paper [16] where it has been shown that this analysis method was very accurate and easy to be employed to analyze more complicated planar ring structures.

In the above mentioned papers, no one has taken into account the thickness of conductor, multiple ring structures, and/or multiple substrate layers. In this paper, we extend the rectangular boundary division method used in the previous paper to analyze very general planar structures taking all of such factors into consideration. The region to be analyzed is divided into subregions of thick-wall cylindrical tubes. Laplace's equation is solved in each region based on the method of the separation of variables. A special application scheme of the boundary condition is devised to decrease the number of necessary equations. The capacitances of several planar ring structures with various conductor thickness are calculated and numerical results are compared with the available numerical data in the zero-thickness conductor limit cases.

II. Extension of Rectangular Boundary Division Method

The rectangular boundary division method has been extensively studied in the quasi-TEM wave analysis of various straight transmission line structures [17]–[18]. It has been recently shown that the method could be easily used to analyze planar ring structures [16]. The only difference between the original and extended one is that Laplace's equation has to be solved in the cylindrical coordinate system and that Bessel functions have to be handled instead of sinusoidal functions.

Fig. 1 shows an example of thick-conductor multiple

Manuscript received October 24, 1991, revised February 20, 1992.

The authors are with the University of Electro-Communications, Department of Electrical Engineering, 1-5-1 Chofugaoka, Chofu, Tokyo 182, Japan.

IEEE Log Number 9202132.

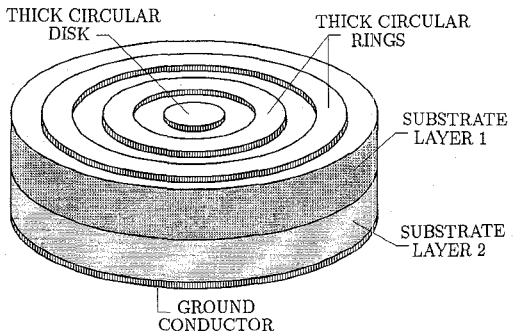

Fig. 1. Multiple planar ring structure with thick conductors on multiple substrate layers.

planar ring structures on multiple substrate layers. The region to be analyzed is divided into subregions of thick-wall cylindrical tubes as shown in Fig. 2(a). Fig. 2(b) shows that the cross-section of the thick-wall tube is composed of a few rectangular subregions. The structure to be analyzed has a metal enclosure, but the dimensions of the side and top wall can be chosen as large enough as open boundary is simulated.

Analytical part of the method is developed for the thick-conductor planar ring whose cross-sectional view together with four divided regions is shown in Fig. 3. The potential for each of the four rectangular regions can be expressed based on the method of the separation of variables as follows:

$$\phi_1(\rho, z) = \sum_{n=1}^{\infty} A_{1n} \sinh(k_{1n} z)\, J_0(k_{1n}\rho) \quad (0 \le \rho \le c;\ 0 \le z \le h) \tag{1a}$$

$$\phi_2(\rho, z) = V_0 + \sum_{n=1}^{\infty} \{A_{2n} \sinh[k_{2n}(z-h)] + B_{2n} \cosh[k_{2n}(z-h)]\} J_0(k_{2n}\rho) \quad (0 \le \rho \le r_1;\ h \le z \le h+t) \tag{1b}$$

$$\phi_3(\rho, z) = V_0 \frac{\ln(c/\rho)}{\ln(c/r_2)} + \sum_{n=1}^{\infty} \{A_{3n} \sinh[k_{3n}(z-h)] + B_{3n} \cosh[k_{3n}(z-h)]\} \cdot [J_0(k_{3n}\rho) + C_{3n} Y_0(k_{3n}\rho)] \quad (r_2 \le \rho \le c;\ h \le z \le h+t) \tag{1c}$$

$$\phi_4(\rho, z) = \sum_{n=1}^{\infty} A_{4n} \sinh[k_{4n}(h+t+h_1-z)] J_0(k_{4n}\rho) \quad (0 \le \rho \le c;\ h+t \le z \le h+t+h_1) \tag{1d}$$

where J_0 and Y_0 denote the 0-th order Bessel functions of the first and the second kind, respectively. $k_{1n}(=k_{4n})$, k_{2n} and k_{3n} are the roots of the following equations:

$$J_0(k_{1n}c) = 0 \tag{2a}$$

$$J_0(k_{2n}r_1) = 0 \tag{2b}$$

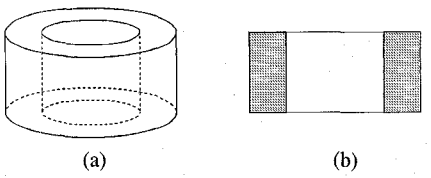

Fig. 2. (a) A thick-wall cylindrical tube as a typical subregion. (b) Rectangular regions in the cross-section of the tube.

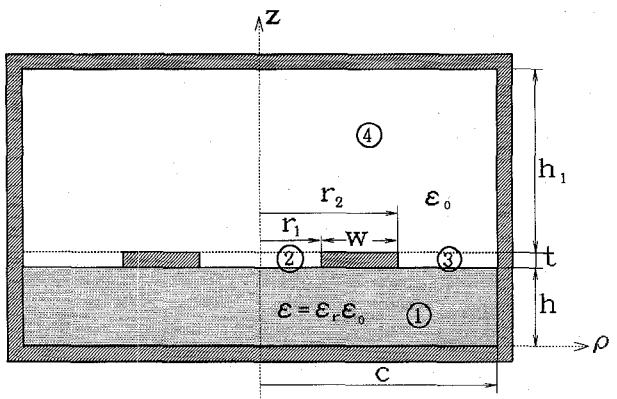

Fig. 3. Cross-sectional view and dimensions of a planar ring with thick conductor and four divided regions.

$$J_0(k_{3n}r_2)\, Y_0(k_{3n}c) - J_0(k_{3n}c)\, Y_0(k_{3n}r_2) = 0 \tag{2c}$$

A_{1n}, A_{2n}, B_{2n}, A_{3n}, B_{3n} and A_{4n} are unknown coefficients. C_{3n} is given by

$$C_{3n} = -\frac{J_0(k_{3n}r_2)}{Y_0(k_{3n}r_2)} = -\frac{J_0(k_{3n}c)}{Y_0(k_{3n}c)} \tag{3}$$

V_0 is the given potential to the planar ring. The boundary conditions for the top and bottom walls have been satisfied in (1a) and (1d).

The summation of the Bessel function in (1c) is in general denoted in the form of a linear combination of Bessel functions as

$$B_m(k_n\rho) = J_m(k_n\rho) + C_n Y_m(k_n\rho). \tag{4}$$

Boundary conditions required for the continuation of the potential functions at each interface can be expressed as follows:

$$\phi_1(\rho, h) = \phi_2(\rho, h) \quad (0 \le \rho \le r_1)$$
$$\phi_1(\rho, h) = \phi_3(\rho, h) \quad (r_2 \le \rho \le c) \tag{5a}$$

$$\phi_2(\rho, h+t) = \phi_4(\rho, h+t) \quad (0 \le \rho \le r_1)$$
$$\phi_3(\rho, h+t) = \phi_4(\rho, h+t) \quad (r_2 \le \rho \le c) \tag{5b}$$

The common and unknown potential functions at the interface $z = h$ and $z = h + t$ are denoted by $f(\rho)$ and $g(\rho)$, respectively. These functions are related to the coefficients of the Fourier series given in (1) using the orthogonality of Bessel functions as

$$A_{1n} = \frac{2}{c^2 \sinh(k_{1n}h)\, J_1^2(k_{1n}c)} \int_0^c \rho f(\rho)\, J_0(k_{1n}\rho)\, d\rho \tag{6a}$$

$$A_{2n} = \frac{2}{r_1^2 J_1^2(k_{2n} r_1)} \left\{ \frac{1}{\sinh(k_{2n} t)} \cdot \left[\int_0^{r_1} \rho g(\rho) J_0(k_{2n}\rho)\, d\rho - V_0 \int_0^{r_1} \rho J_0(k_{2n}\rho)\, d\rho \right] - \frac{1}{\tanh(k_{2n} t)} \left[\int_0^{r_1} \rho f(\rho) J_0(k_{2n}\rho)\, d\rho - V_0 \int_0^{r_1} \rho J_0(k_{2n}\rho)\, d\rho \right] \right\} \quad (6b)$$

$$B_{2n} = \frac{2}{r_1^2 J_1^2(k_{2n} r_1)} \left[\int_0^{r_1} \rho f(\rho) J_0(k_{2n}\rho)\, d\rho - V_0 \int_0^{r_1} \rho J_0(k_{2n}\rho)\, d\rho \right] \quad (6c)$$

$$A_{3n} = \frac{2}{c^2 B_1^2(k_{3n} c) - r_2^2 B_1^2(k_{3n} r_2)} \cdot \left\{ \frac{1}{\sinh(k_{3n} t)} \left[\int_{r_2}^{c} \rho g(\rho) B_0(k_{3n}\rho)\, d\rho - \frac{V_0}{\ln(c/r_2)} \int_{r_2}^{c} \rho \ln(c/\rho) B_0(k_{3n}\rho)\, d\rho \right] - \frac{1}{\tanh(k_{3n} t)} \left[\int_{r_2}^{c} \rho f(\rho) B_0(k_{3n}\rho)\, d\rho - \frac{V_0}{\ln(c/r_2)} \int_{r_2}^{c} \rho \ln(c/\rho) B_0(k_{3n}\rho)\, d\rho \right] \right\} \quad (6d)$$

$$B_{3n} = \frac{2}{c^2 B_1^2(k_{3n} c) - r_2^2 B_1^2(k_{3n} r_2)} \cdot \left[\int_{r_2}^{c} \rho f(\rho) B_0(k_{3n}\rho)\, d\rho - \frac{V_0}{\ln(c/r_2)} \int_{r_2}^{c} \rho \ln(c/\rho) B_0(k_{3n}\rho)\, d\rho \right] \quad (6e)$$

$$A_{4n} = \frac{2}{c^2 \sinh(k_{4n} h_1) J_1^2(k_{4n} c)} \int_0^{c} \rho f(\rho) J_0(k_{4n}\rho)\, d\rho \quad (6f)$$

The unknown potential functions for the interfaces are now approximated with a linear combination of the spline functions as

$$f(\rho) = \sum_{i=0}^{m} p_i F_i(\rho) \quad (7a)$$

$$g(\rho) = \sum_{i=0}^{m} q_i F_i(\rho) \quad (7b)$$

where

$$F_i(\rho) = \begin{cases} \dfrac{\rho - \rho_{i-1}}{\rho_i - \rho_{i-1}} & (\rho_{i-1} \le \rho \le \rho_i) \\ \dfrac{\rho_{i+1} - \rho}{\rho_{i+1} - \rho_i} & (\rho_i \le \rho \le \rho_{i+1}) \\ 0 & (\text{elsewhere}) \end{cases} \quad (8)$$

is the first-order spline function, and p_i, and q_i ($i = 0, \cdots, m$) are spline parameters. The unknown coefficients in (6a) through (6f) can be expressed in terms of p_i and q_i. The total electric field energy in the structure is expressed as

$$U = 2\pi \sum_{k=1}^{4} \frac{1}{2} \epsilon_k \iint_{S_k} \left\{ \left(\frac{\partial \phi_k}{\partial \rho} \right)^2 + \left(\frac{\partial \phi_k}{\partial z} \right)^2 \right\} \rho\, d\rho\, dz \quad (9)$$

where ϵ_k and S_k denote the dielectric permittivity and the cross-sectional area of the region k ($k = 1, 2, 3$ and 4). Carrying out the integration given in (6), and substituting them in (1) and (9), the total electric field energy is rewritten as

$$U = \frac{\epsilon_0 V_0^2 t}{2 \ln(c/r_2)} + \sum_{i=0}^{M} \sum_{j=0}^{M} K_{ij} x_i x_j \quad (10)$$

where $M = 2m + 1$, $x_i = \{p_0, p_1, \cdots, p_m, q_0, q_1, \cdots, q_m\}$. Newly introduced coefficients K_{ij} ($i, j = 0, 1, 2, \cdots, M$) are given in Appendix.

The remaining boundary condition, the continuity of the normal electric flux, is satisfied by taking the minimum of the total electric field energy as

$$\frac{\partial U}{\partial p_i} = 0 \qquad (i = 0, 1, \cdots, m;\ i \ne s, s+1) \quad (11a)$$

$$\frac{\partial U}{\partial q_i} = 0 \qquad (i = 0, 1, \cdots, m;\ i \ne s, s+1) \quad (11b)$$

where $p_s = x_s$, $p_{s+1} = x_{s+1}$, $q_s = x_{m+s}$ and $q_{s+1} = x_{m+s+1}$ are the known potentials on the conductors. These conditions result in a set of linear inhomogeneous simultaneous equations of the spline parameters as

$$\sum_{j \ne \{Q\}} K_{ij} x_j = -\sum_{j=s}^{s+1} K_{ij} x_j - \sum_{j=m+s}^{m+s+1} K_{ij} x_j \qquad (i = 0, 1, \cdots, M;\ i \notin \{Q\}) \quad (12)$$

where $\{Q\} = \{s, s+1, m+s, m+s+1\}$. The capacitance produced by the structure is readily given by equating the energy expression stored in a capacitor and U as

$$C = \frac{2U}{V_0^2}. \quad (13)$$

III. Numerical Results

Since the number of Fourier series terms, n, and the number of spline knots, m, are unknown finite values in our numerical processing, convergence property against n and m has been tested firstly. The rapid change of electric fields near the conductor edges is taken into account by a nonuniform discretization procedure. The side and top walls are kept at far distances, $c = 2r_2 + 10h$ and $h_1 = 100\ h$, respectively, in order to make their influence on capacitance values negligible. Fig. 4(a) and Fig. 4(b) show the convergence of the normalized capacitance values with respect to n and m, respectively, for three kinds of structures, where the circular disk is defined by setting $r_1 = 0$ and $r_2 = a$. These results indicate that satisfactory numbers for convergence are in the ranges given by $n \geq 500$ and $m \geq 35$. The indicated number of spline knots in Fig. 4 is for zero-thickness conductor structures. Therefore, this number is doubled for structures with thick-conductor. In general, the convergence property depends on the normalized dimensions, t/c, h/c, w/c, and r_2/c, where $w = r_2 - r_1$. In our examples, we have set as $n = 1000$ and $m = 40$. Typical computation time for one capacitance value is about 20 seconds for zero-thickness conductor structures and about 65 seconds for thick-conductor structures on a SUN-4 workstation.

The problem of circular disks with zero-thickness conductor has been extensively studied by many authors and exact numerical results for the capacitances have been already given. The most exact results for the capacitance of a circular disk seem to have been given in the references [5]–[7]. Our numerical results for the capacitance of circular disks with zero-thickness conductor agree well with those given in the references [5]–[7], as indicated in Fig. 5 where the normalized capacitance $Ch/\pi\epsilon_0\epsilon_r a^2$ is shown against the normalized substrate thickness, h/a. This fact confirms the exactness of our method in the zero-thickness limit. Fig. 5 also includes curves showing the influence of the conductor thickness. The conductor thickness has a significant effect on the capacitance values for the cases where fringing fields are prominent as expected.

The presence of the ground conductor on the upper surface of the substrate also has a significant influence on the capacitance of circular disks. Fig. 6 shows the normalized capacitance of a disk against the separation between the disk and the ground conductor on the substrate both for zero-thickness and thick conductors. This thickness effect has not been treated until now, to the authors' knowledge, but can be analyzed with our method. We can also predict the influence of a side wall. This influence is weak for $s/h \geq 10$, and keeping the side wall at distance $c = 2a + 10h$ is quite reasonable for simulating an open boundary.

Although the direct knowledge of the charge distribution is not required in our calculation of the capacitance, we can estimate the charge distribution by solving a set of linear inhomogeneous equations and by going back to (1) to find the potential and electric field in the region.

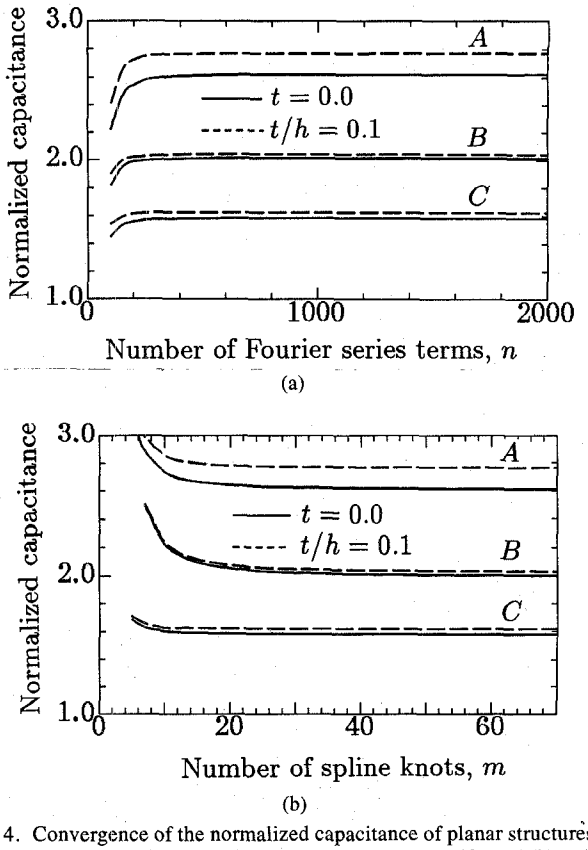

Fig. 4. Convergence of the normalized capacitance of planar structures (a) against the number of the Fourier series terms, n ($m = 40$) and (b) against the number of the spline knots, m ($n = 1000$). Structure A: Disk, $a/h = 1.0$, $\epsilon_r = 2.65$. Structure B: Ring, $r_1/h = 5.0$, $r_2/h = 6.0$, $\epsilon_r = 9.6$. Structure C: Disk, $a/h = 5.0$, $\epsilon_r = 1.0$.

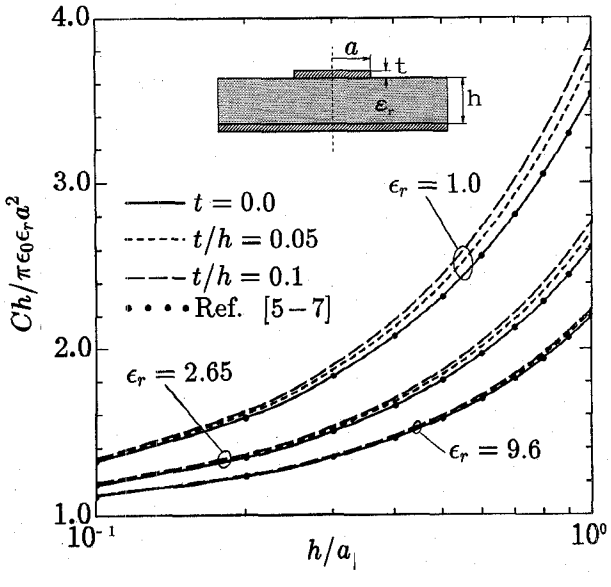

Fig. 5. Normalized capacitance of a thick circular disk against the normalized substrate thickness.

Gate or Maxwell functions as the extreme case are usually used for the charge distribution as basis in the spectral domain analysis. It has been shown that neither of these basis gives good results for intermediate sizes [4], and therefore, a combination of these two extreme functions is needed [8]. We have calculated the charge distribution

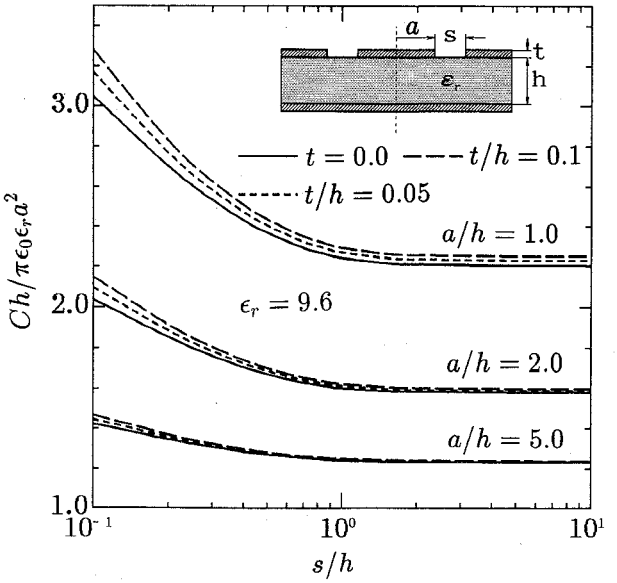

Fig. 6. Normalized capacitance of a thick circular disk near the ground conductor on the substrate as a function of the separation.

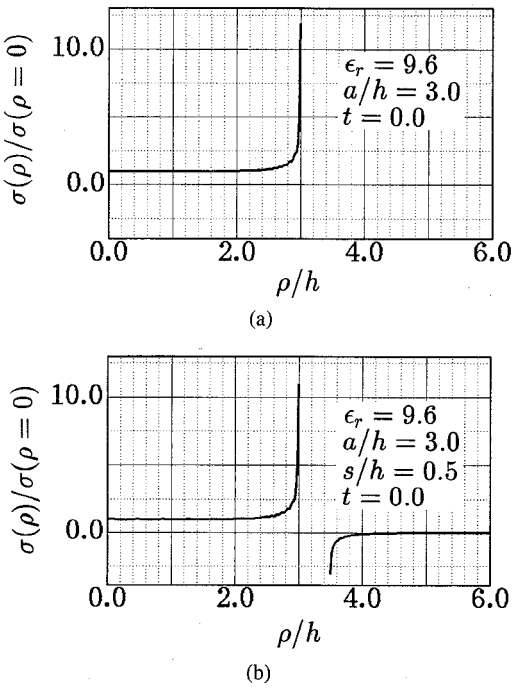

Fig. 7. Normalized charge distribution (a) of a circular disk and (b) of a circular disk near the ground conductor on the substrate.

for the intermediate case as $a/h = 3.0$, $t = 0$ without any difficulty and numerical results are shown in Fig. 7(a). Fig. 7(b) shows the influence of the existence of the ground conductor near the disk on the charge distribution.

The fringing field of a planar ring is different depending on whether the position is inside or outside of the ring since electric charge is asymmetrically distributed about the mean radius of the ring. This fact is also very difficult to be incorporated into the spectral domain analysis because the extent of the asymmetry depends on the curvature radius. The coupling between the field at one point of the ring to that at the other point of diametrical opposition is different depending on whether the point is inside or outside of the ring. The outside fringing field resembles the fringing field of a degenerated microstrip line and the inside one that of degenerated coupled lines. Bedair [10] has calculated the capacitance of a planar ring giving good results in the case of wide rings, and has given an explicit approximation formula. Fig. 8 shows the normalized capacitance, $Ch/\pi\epsilon_0\epsilon_r(r_2^2 - r_1^2)$, of a planar ring as a function of the curvature radius. Significant differences have been found between our results for zero-thickness rings and the results given by [10], for small values of inner radius. The curvature effect on the capacitance of thick rings is similar to that of the capacitance of zero-thickness rings. When a conductor is the thicker, fringing fields are the more prominent.

The influence of the ground conductors on the substrate on the capacitance of a planar ring has been also studied. Such ground conductors can be placed in the structure in three ways. One way we had treated in a previous paper is called a coplanar circular ring, where a planar ring has the ground conductor on both sides as shown in Fig. 9. Other two ways have the ground conductor outside, as shown in Fig. 10, or inside, as shown in Fig. 11. The

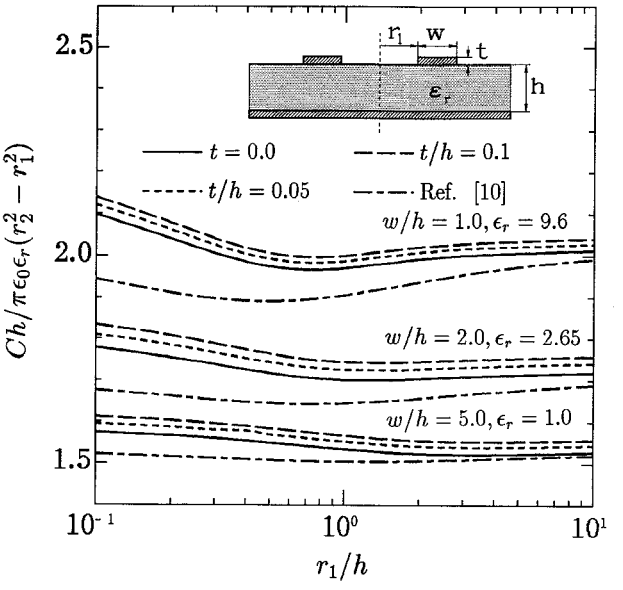

Fig. 8. Normalized capacitance of a thick planar ring.

normalized capacitance of the planar ring is also shown in Fig. 10 and Fig. 11 as the function of the separation between the ring and the ground conductor on the substrate.

Again, zero-thickness and thick conductor structures are treated for rings with the same mean radius, $r_m/h = 5.0$. Although the curves show the same trend in these three cases, the extent of influence is different depending on the case. It is of interest to know that the influence depends on whether one conductor is situated outside or inside the circular ring. When the conductor is inserted inside the ring, the curvature effect is weakened. The thickness of

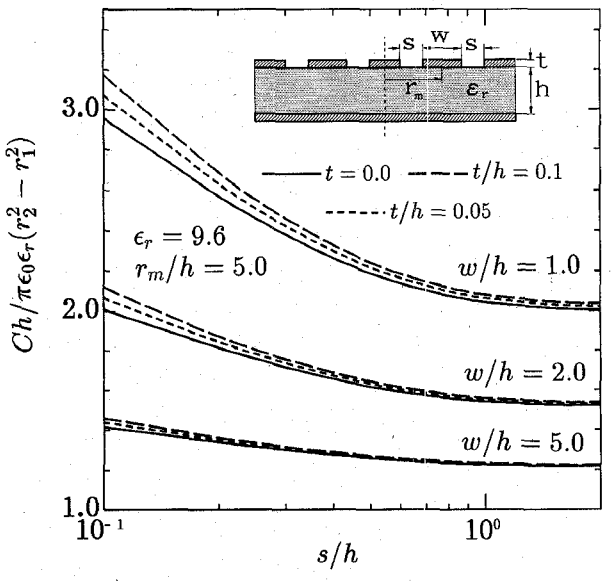

Fig. 9. Normalized capacitance of a coplanar ring as a function of the separation.

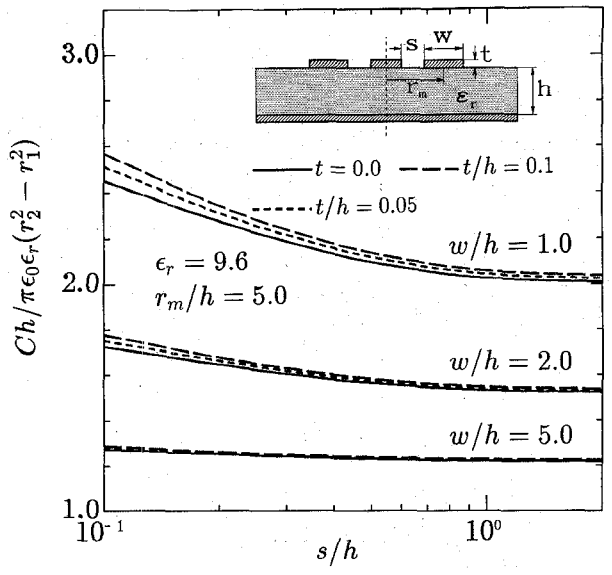

Fig. 11. Normalized capacitance of a planar ring near the inside ground conductor on the substrte as a function of the separation.

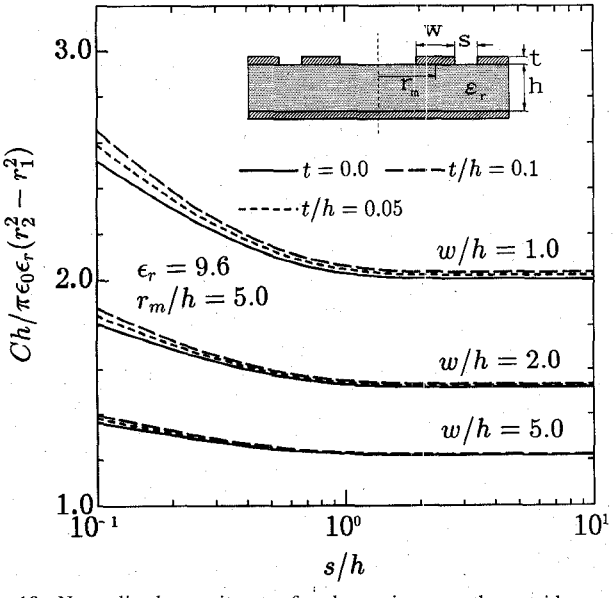

Fig. 10. Normalized capacitance of a planar ring near the outside ground conductor on the substrate as a function of the separation.

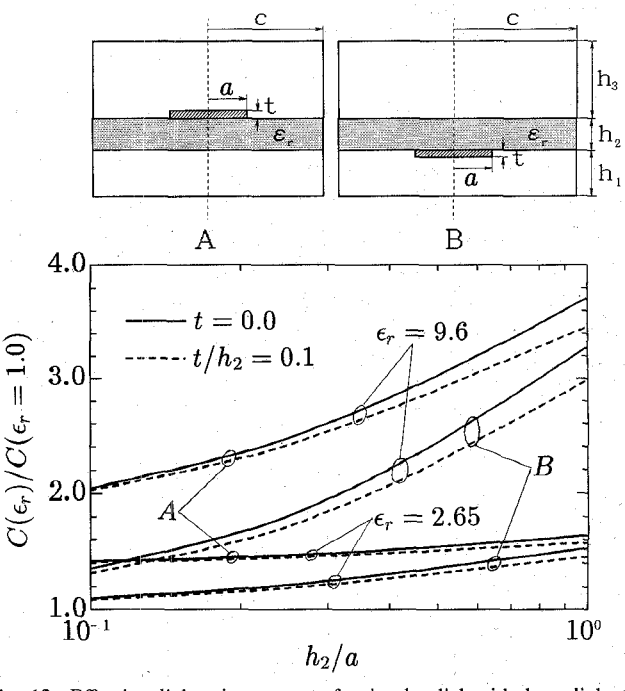

Fig. 12. Effective dielectric constant of a circular disk with three dielectric layers, $h_1 = h_2$, $h_3 = 10h_2$, $c = 2a + 10h_2$.

the conductor has a strong effect on the fields for small separation, since the electric field is more concentrated between the conductors. As separation is increased, the capacitance value naturally approaches the capacitance value of an isolated planar ring in all cases.

Next, we analyze the planar ring and circular disk structures in three dielectric layers choosing similar examples presented in Fig. 12 and Fig. 13. It is possible by using this analysis method to calculate the effective dielectric constant, i.e. the ratio of the capacitance with the presence of dielectrics to the capacitance without the presence of dielectrics. Mathematical expressions for calculating the capacitance of these structures are more extensive because more divided regions must be used. Fig. 12 and Fig. 13 show the effective dielectric constant of the circular disk and ring, respectively, with three dielectric layers in two configurations. It is known that the electric field is mostly concentrated in the air regions for this kind of structures, so that only values close to one as the effective dielectric constants are obtained. The effect of the conductor thickness can not be neglected anymore as seen from these figures. In practice, these structures usually have grooves or pedestals to support the substrate, and those additional structures can be easily incorporated into our calculation.

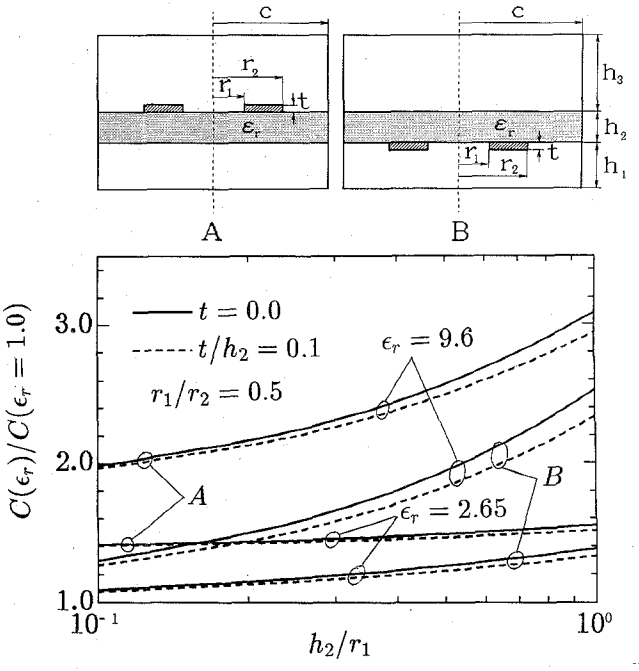

Fig. 13. Effective dielectric constant of a planar ring with three dielectric layers, $h_1 = h_2$, $h_3 = 10h_2$, $c = 2r_2 + 10h_2$.

IV. Conclusion

An effective analysis method was presented which was devised for calculating the capacitances of multiple planar ring structures with thick conductors on multiple substrate layers. Attention was specially paid to the effects of the conductor thickness and of the presence of the ground conductor on the substrate on the capacitance values. The calculated values of the capacitance of circular disks showed good agreement with other available data in the zero-thickness limit. The capacitance values of planar rings also agreed well with capacitance values calculated based on the past approximate formulas for wide rings. The capacitances of the structures with three dielectric layers were also calculated for both circular disks and planar rings in two configurations.

The merits of our method are: 1) generality and easiness to be employed in the analysis of complicated planar structures, 2) simple integrals in the closed form involved in the analytical part of the method, 3) no necessity of a prior knowledge of charge distributions on conductors, 4) only the necessity of potential specification to conductors in the case of multiple conductors, and 5) very accurate numerical results with relatively small computational time and memory capacity. The conductor-thickness of circular disks and planar rings has been taken into account, to the authors' knowledge, for the first time in the analysis with a rigorous treatment and a variety of numerical examples.

Appendix

The coefficient K_{ij} in (12) is defined as

$$K_{ij} = K_{1ij} + K_{2ij} + K_{3ij} + K_{4ij}$$
$$K_{ij} = K_{ji} \tag{A1}$$

where

$$K_{1ij} = \begin{cases} \sum_{n=1}^{\infty} H_{1n} I_{1ni} I_{1nj} & (0 \le i, j \le M_2) \\ 0 & \text{(elsewhere)} \end{cases} \tag{A2a}$$

$$K_{2ij} = \begin{cases} \sum_{n=1}^{\infty} H_{2n} I_{2ni} I_{2nj} & (0 \le i, j \le M_1) \\ \sum_{n=1}^{\infty} -H'_{2n} I_{2ni} I'_{2nj} & (0 \le i \le M_1,\ M_2 + 1 \le j \le M_3) \\ \sum_{n=1}^{\infty} H_{2n} I'_{2ni} I'_{2nj} & (M_2 + 1 \le i, j \le M_3) \\ 0 & \text{(elsewhere)} \end{cases} \tag{A2b}$$

$$K_{3ij} = \begin{cases} \sum_{n=1}^{\infty} H_{3n} I_{3ni} I_{3nj} & (M_1 + 1 \le i, j \le M_2) \\ \sum_{n=1}^{\infty} -H'_{3n} I_{3ni} I'_{3nj} & (M_1 + 1 \le i \le M_2,\ M_3 + 1 \le j \le M) \\ \sum_{n=1}^{\infty} H_{3n} I'_{3ni} I'_{3nj} & (M_3 + 1 \le i, j \le M) \\ 0 & \text{(elsewhere)} \end{cases} \tag{A2c}$$

$$K_{4ij} = \begin{cases} \sum_{n=1}^{\infty} H_{4n} I'_{4ni} I'_{4nj} & (M_2 + 1 \le i, j \le M) \\ 0 & \text{(elsewhere)} \end{cases} \tag{A2d}$$

$$M_1 = s,\ M_2 = m,\ M_3 = m + s + 1,\ M = 2m + 1.$$

$$I_{1ni} = \begin{cases} -\dfrac{\alpha(k_{1n}, \rho_1) - \alpha(k_{1n}, \rho_0)}{k_{1n}(\rho_1 - \rho_0)} & i = 0 \\ \dfrac{\alpha(k_{1n}, \rho_i) - \alpha(k_{1n}, \rho_{i-1})}{k_{1n}(\rho_i - \rho_{i-1})} - \dfrac{\alpha(k_{1n}, \rho_{i+1}) - \alpha(k_{1n}, \rho_i)}{k_{1n}(\rho_{i+1} - \rho_i)} & i = 1, \cdots, m \end{cases} \tag{A3a}$$

$$I_{2ni} = \begin{cases} -\dfrac{\alpha(k_{2n}, \rho_1) - \alpha(k_{2n}, \rho_0)}{k_{2n}(\rho_1 - \rho_0)} & i = 0 \\ \dfrac{\alpha(k_{2n}, \rho_i) - \alpha(k_{2n}, \rho_{i-1})}{k_{2n}(\rho_i - \rho_{i-1})} - \dfrac{\alpha(k_{2n}, \rho_{i+1}) - \alpha(k_{2n}, \rho_i)}{k_{2n}(\rho_{i+1} - \rho_i)} & i = 1, \cdots, s-1 \\ \dfrac{\alpha(k_{2n}, \rho_s) - \alpha(k_{2n}, \rho_{s-1})}{k_{2n}(\rho_s - \rho_{s-1})} & i = s \end{cases} \tag{A3b}$$

$$I_{3ni} = \begin{cases} -\dfrac{\beta(k_{3n}, \rho_{s+2}) - \beta(k_{3n}, \rho_{s+1})}{k_{3n}(\rho_{s+2} - \rho_{s+1})} & i = s + 1 \\ \dfrac{\beta(k_{3n}, \rho_i) - \beta(k_{3n}, \rho_{i-1})}{k_{3n}(\rho_i - \rho_{i-1})} - \dfrac{\beta(k_{3n}, \rho_{i+1}) - \beta(k_{3n}, \rho_i)}{k_{3n}(\rho_{i+1} - \rho_i)} & i = s + 2, \cdots, m \end{cases} \tag{A3c}$$

Non-primed and primed I_{ni}-coefficients in (A.2) are related to the distribution of discretization points on the interfaces, at $z = h$ and at $z = h + t$, respectively. In the present case, it was natural to use similar discretization points at both interfaces. Therefore, $I'_{2ni} = I_{2ni}$, $I'_{3ni} = I_{3ni}$ and $I'_{4ni} = I_{1ni}$.

$$\alpha(k_n, \rho_i) = k_n \rho_i J_0(k_n \rho_i) - S_0(k_n \rho_i)$$

$$S_0(k_n \rho_i) = \int_0^{\rho_i} J_0(k_n \rho)\, d\rho = 2 \sum_{j=0}^{\infty} J_{2j+1}(k_n \rho_i) \tag{A4a}$$

$$\beta(k_n, \rho_i) = k_n \rho_i B_0(k_n \rho_i) - I_0(k_n \rho_i)$$

$$I_0(k_n \rho_i) = \int_0^{\rho_i} B_0(k_n \rho)\, d\rho = 2 \sum_{j=0}^{\infty} B_{2j+1}(k_n \rho_i) \tag{A4b}$$

$$H_{1n} = \frac{\epsilon_1 c}{(k_{1n} c)^3 J_1^2(k_{1n} c) \tanh (k_{1n} h)} \tag{A5a}$$

$$H_{2n} = \frac{\epsilon_2 r_1}{(k_{2n} r_1)^3 J_1^2(k_{2n} r_1) \tanh (k_{2n} t)} \tag{A5b}$$

$$H'_{2n} = \frac{\epsilon_2 r_1}{(k_{2n} r_1)^3 J_1^2(k_{2n} r_1) \sinh (k_{2n} t)} \tag{A5c}$$

$$H_{3n} = \frac{\epsilon_3 c}{(k_{3n} c)^3 [B_1^2(k_{3n} c) - (r_2/c)^2 B_1^2(k_{3n} r_2)] \tanh (k_{3n} t)} \tag{A5d}$$

$$H'_{3n} = \frac{\epsilon_3 c}{(k_{3n} c)^3 [B_1^2(k_{3n} c) - (r_2/c)^2 B_1^2(k_{3n} r_2)] \sinh (k_{3n} t)} \tag{A5e}$$

$$H_{4n} = \frac{\epsilon_4 c}{(k_{4n} c)^3 J_1^2(k_{4n} c) \tanh (k_{4n} h_1)} \tag{A5f}$$

where $\epsilon_1 = \epsilon_r \epsilon_0$ and $\epsilon_2 = \epsilon_3 = \epsilon_4 = \epsilon_0$.

The summations, S_0 and I_0, in (A4) are carried out by using the recurrence relations [19] and the polynomial approximations [20].

ACKNOWLEDGMENT

The authors wish to thank Professor K. Atsuki of the University of Electro-communication for his helpful comments and discussions.

REFERENCES

[1] T. Itoh and R. Mittra, "A new method for calculating the capacitance of a circular disk for microwave integrated circuits," *IEEE Trans. Microwave Theory Tech.*, vol. 21, pp. 431–432, June 1973.

[2] ——, "Analysis of a microstrip disk resonator," AEÜ 27, pp. 456–458, 1973.

[3] S. R. Borkar and R. F. H. Yang, "Capacitance of a circular disk for application in microwave integrated circuits," *IEEE Trans. Microwave Theory Tech.*, vol. 23, pp. 588–591, July 1975.

[4] S. Coen and G. M. L. Gladwell, "A Legendre approximation method for the circular microstrip disk problem," *IEEE Trans. Microwave Theory Tech.*, vol. 25, pp. 1-6, Jan. 1977.
[5] W. C. Chew and J. A. Kong, "Effects of fringing fields on the capacitance of circular microstrip disk," *IEEE Trans. Microwave Theory and Tech.*, vol. 28, pp. 98-103, Feb. 1980.
[6] K. Hongo and T. Takahashi, "Evaluation of the integrals occurring in the study of circular microstrip disk," *IEEE Trans. Microwave Theory Tech.*, vol. 30, pp. 1279-1282, Aug. 1982.
[7] M. S. Leong, P. S. Kooi, and K. P. Yeo, "Capacitance of a circular disc for applications in microwave integrated circuits," *IEE Proc. H, Microwave, Opt. & Antennas*, vol. 128, pp. 320-322, Dec. 1981.
[8] M. S. Leong, P. S. Kooi, and K. P. Yeo, "Determination of circular microstrip Disc by Nobles's Variational Method," *IEE Proc. H, Microwave, Opt. & Antennas*, vol. 128, pp. 306-310, Dec. 1981.
[9] I. Wolf and N. Knoppik, "Rectangular and circular microstrip disk capacitors and resonators," *IEEE Trans. Microwave Theory Tech.*, vol. 22, pp. 857-864, Oct. 1974.
[10] S. S. Bedair, "Closed form expressions for the static capacitances of some microstrip disk capacitors," AEÜ 39, pp. 269-272, 1985.
[11] W. C. Chew and J. A. Kong, "Microstrip capacitance for a circular disk through matched asymptotic expansions," *SIAM J. Appl. Math.*, vol. 42, pp. 302-317, Apr. 1982.
[12] H. A. Wheeler, "A simple formula for the capacitance of a disc on dielectric on a plane," *IEEE Trans. Microwave Theory Tech.*, vol. 30, pp. 2050-2054, Nov. 1982.
[13] E. F. Kuester, "Explicit approximations for the static capacitance of a microstrip patch of arbitrary shape," *J. Electromagnetic Waves and Applications*, vol. 2, no. 1, pp. 103-135, 1987.
[14] A. K. Sharma and B. Bhat, "Spectral domain analysis of microstrip ring resonators," *AEÜ 33*, pp. 130-132, 1979.
[15] A. K. Sharma and B. Bhat, "Influence of a shielding on the capacitance of microstrip disk and ring structures," AEÜ 34, pp. 41-44, 1980.
[16] F. Tefiku and E. Yamashita, "Accurate calculation method for the capacitance of generalized circular structures," *Int. J. Microwave and Millimeter-Wave Computer-Aided Engineering*, vol. 2, no. 1, pp. 4-11, Jan. 1992.
[17] E. Yamashita, M. Nakajima, and K. Atsuki, "Analysis method for generalized suspended striplines," *IEEE Trans. Microwave Theory Tech.*, vol. 34, pp. 1457-1463, Dec. 1986.
[18] E. Yamashita, K. R. Li, and Y. Suzuki, "Characterization method and simple design formulas of MCS lines proposed for MMIC's," *IEEE Trans. Microwave Theory Tech.*, vol. 35, pp. 1355-1362, Dec. 1987.
[19] G. N. Watson, *A Treatise on Theory of Bessel Functions*. London: Cambridge, 1966.
[20] M. Abramowitz and I. A. Stegun, Ed., *Handbook of Mathematical Functions with Formulas, Graphs and Mathematical Tables*. New York: Dover, 1964.

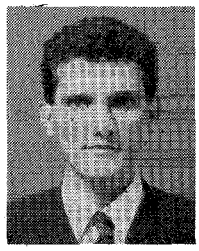

Faton Tefiku (SM'91) was born in Kosovo Province, Yugoslavia, in 1958. He received the B.S. degree from the University of Prishtina, in June 1981, and the M.S. degree from the University of Zagreb, Croatia, in June 1987, both in electrical engineering.

In 1982 he joined the Faculty of Electrical Engineering, University of Prishtina, Kosovo, as Research Assistant. From April, 1990, he has been with the University of Electro-Communications, Tokyo, Japan, where he is currently working toward the Ph.D. degree. His current research interest includes the numerical analysis of microwave and millimeter wave planar circuits and transmission lines.

Eikichi Yamashita (M'66-SM'69-F'84) was born in Tokyo, Japan, on February 4, 1933. He received the B.S. degree from the University of Electro-communications, Tokyo, Japan, and the M.S. and Ph.D. degree from the University of Illinois, Urbana, all in electrical engineering, in 1956, 1963, and 1966, respectively.

From 1956 to 1964, he was a member of the research staff on millimeter-wave engineering at the Electrotechnical Laboratory, Tokyo, Japan. While on leave from 1961 to 1963 and from 1964 to 1966, he studied solid-state devices in the millimeter-wave region at the Electro-Physics Laboratory, University of Illinois. He became Associate Professor in 1967 and Professor in 1977 in the Department of Electronic Engineering, the University of Electro-communications, Tokyo, Japan. His research work since 1956 has been principally on applications of electromagnetic waves such as various microstrip transmission lines, wave propagation in gaseous plasma, pyroelectric-effect detectors in the submillimeter-wave region, tunnel-diode oscillators, wide-band laser modulators, various types of optical fibers, and ultra-short electrical pulse propagation on transmission lines.

Dr. Yamashita was Chairperson of the Technical Group on Microwaves, IEICE, Japan, for the period 1985-1986 and Vice-Chairperson, Steering Committee, Electronics Group, IEICE, for the period 1989-1990. He served as Associate Editor of the IEEE TRANSACTIONS ON MICROWAVE THEORY AND TECHNIQUES during the period 1980-1984. He was elected Chairperson of the MTT-S Tokyo Chapter for the period 1985-1986. He served as Chairperson of International Steering Committee, 1990 Asia-Pacific Microwave Conference, held in Tokyo. He edited the book, *Analysis Methods for Electromagnetic Wave Problems*, published by Artech House.